An oxysterol biomarker for 7-dehydrocholesterol oxidation in cell/mouse models for Smith-Lemli-Opitz syndrome[S]

Libin Xu,[1,*] Zeljka Korade,[1,†] Dale A. Rosado, Jr.,[*] Wei Liu,[*] Connor R. Lamberson,[*] and Ned A. Porter[2,*]

Department of Chemistry and Vanderbilt Institute of Chemical Biology,* Department of Psychiatry and Vanderbilt Kennedy Center for Research on Human Development,† Vanderbilt University, Nashville, TN 37235

Abstract **The level of 7-dehydrocholesterol (7-DHC) is elevated in tissues and fluids of Smith-Lemli-Opitz syndrome (SLOS) patients due to defective 7-DHC reductase. Although over a dozen oxysterols have been identified from 7-DHC free radical oxidation in solution, oxysterol profiles in SLOS cells and tissues have never been studied. We report here the identification and complete characterization of a novel oxysterol, 3β,5α-dihydroxycholest-7-en-6-one (DHCEO), as a biomarker for 7-DHC oxidation in fibroblasts from SLOS patients and brain tissue from a SLOS mouse model. Deuterated (d_7)-standards of 7-DHC and DHCEO were synthesized from d_7-cholesterol. The presence of DHCEO in SLOS samples was supported by chemical derivatization in the presence of d_7-DHCEO standard followed by HPLC-MS or GC-MS analysis. Quantification of cholesterol, 7-DHC, and DHCEO was carried out by isotope dilution MS with the d_7-standards. The level of DHCEO was high and correlated well with the level of 7-DHC in all samples examined ($R = 0.9851$).** **Based on our in vitro studies in two different cell lines, the mechanism of formation of DHCEO that involves 5α,6α-epoxycholest-7-en-3β-ol, a primary free radical oxidation product of 7-DHC, and 7-cholesten-3β,5α,6β-triol is proposed. In a preliminary test, a pyrimidinol antioxidant was found to effectively suppress the formation of DHCEO in SLOS fibroblasts.**—Xu, L., Z. Korade, D. A. Rosado, Jr., W. Liu, C. R. Lamberson, and N. A. Porter. **An oxysterol biomarker for 7-dehydrocholesterol oxidation in cell/mouse models for Smith-Lemli-Opitz syndrome.** ***J. Lipid Res.*** **2011.** 52: **1222–1233.**

Supplementary key words free radical oxidation • lipid peroxidation • metabolism • oxidative stress • antioxidant

Smith-Lemli-Opitz syndrome (SLOS) is a metabolic disorder resulting from mutations in the gene encoding 7-dehydrocholesterol reductase (DHCR7), the enzyme that catalyzes the reduction of 7-dehydrocholesterol (7-DHC) to cholesterol (Chol) (1–7). Elevated levels of 7-DHC and reduced levels of Chol are observed in tissues and fluids of patients with SLOS due to this enzymatic defect. SLOS is characterized by a broad spectrum of phenotypes including multiple congenital malformations and mental retardation (6, 8–10).

We reported previously that 7-DHC has the highest measured propagation rate constant known for any lipid toward free radical chain oxidation (11). The rate constant determined for the propagation step in 7-DHC autoxidation (2260 $M^{-1}s^{-1}$) is some 200 times that determined for Chol (11 $M^{-1}s^{-1}$) and more than 10 times that of arachidonic acid (197 $M^{-1}s^{-1}$), a polyunsaturated fatty acid that is considered to be highly susceptible to free radical oxidation. In a subsequent report, over a dozen oxysterols were isolated and characterized from 7-DHC free radical oxidation reactions and a reasonable mechanism involving abstraction of hydrogen atoms at C-9 and/or C-14 was proposed to account for the profile of products formed (12). Due to its high oxidizability, substantially more oxidation products

This work was supported by the National Institutes of Health (ES013125) (HD064727), the National Science Foundation (CHE 0717067), and the Vanderbilt Center for Molecular Toxicology Center Grant NIH P30 ES000267. Its contents are solely the responsibility of the authors and do not necessarily represent the official views of the National Institutes of Health or other granting agencies. Z.K. appreciates support from the Vanderbilt Kennedy Center for Research on Human Development.

Manuscript received 1 February 2011 and in revised form 6 March 2011.

Published, JLR Papers in Press, March 14, 2011
DOI 10.1194/jlr.M014498

Abbreviations: APCI, atmospheric pressure chemical ionization; Chol, cholesterol; 7-DHC, 7-dehydrocholesterol; **DHCAO**, 3β,5α-dihydroxy-cholestan-6-one; **DHCEO**, 3β,5α-dihydroxycholest-7-en-6-one; Dhcr7 or DHCR7, 7-dehydrocholesterol reductase; DNPH, 1,4-dinitrophenyl hydrazine; E20, embryonic day 20; Het, heterozygous; HF, human fibroblast; KO, knockout; NP, normal phase; RP, reverse phase; SLOS, Smith-Lemli-Opitz syndrome; SRM, selective reaction monitoring; UV, ultraviolet; WT, wild type.

[1] L. Xu and Z. Korade contributed equally to the manuscript.
[2] To whom correspondence should be addressed.
e-mail: n.porter@vanderbilt.edu

[S] The online version of this article (available at http://www.jlr.org) contains supplementary data in the form of nine figures and supplementary data and references.

would be formed by free radical oxidation of 7-DHC than would be formed from Chol, given comparable levels of the two sterols and an otherwise similar biological environment.

Oxysterols as a class can exert a variety of biological activities including cytotoxicity (13, 14), regulation of Chol homeostasis (14–19), suppression of the immune response (20–23), and interaction with the hedgehog-signaling pathway (24–26). Most of the known oxysterols are formed from Chol by enzymatic or free radical oxidation (i.e., autoxidation), but other sterols also can be subject to oxidation when elevated levels are present (18), such as in various Chol biosynthesis disorders, including SLOS (9). Accumulation of the highly oxidizable 7-DHC in SLOS patients provides an ideal biological environment for oxysterol formation. However, 7-DHC-derived oxysterols have not been analyzed previously in cells from SLOS patients or tissues from SLOS animal models.

Our previous studies showed that the oxysterol mixture derived from 7-DHC free radical oxidation is biologically active and leads to morphological changes in Neuro2a cells treated with these oxysterols (27). The 7-DHC-derived oxysterols were found to reduce cell viability in a dose- and time-dependent manner at sub-μM to μM concentrations and the 7-DHC oxysterol mixture also triggers the same gene expression changes in normal Neuro2a cells that were previously observed in *Dhcr7*-deficient Neuro2a cells. Among the genes most affected are those involved in lipid biosynthesis and cell proliferation.

We undertook the current study to determine if 7-DHC-derived oxysterols are present in SLOS cells and tissues and report here: *1*) the HPLC-MS profiles of oxysterols found in human SLOS fibroblasts and in brains of *Dhcr7*-knockout (KO) mice; *2*) the complete characterization and quantification of a novel oxysterol, 3β,5α-dihydroxycholest-7-en-6-one (**DHCEO**), found in SLOS cell and mouse models using a synthetic deuterated standard; *3*) evidence related to the mechanism of formation of **DHCEO** in human fibroblasts (HFs) and Neuro2a cells; and *4*) studies on the efficacy of a novel antioxidant in suppressing the formation of **DHCEO** in SLOS HFs.

MATERIALS AND METHODS

Materials

[25,26,26,26,27,27,27-d_7]Cholesterol (99% D) was purchased from Medical Isotopes, Inc. Chromium hexacarbonyl (99%) and ruthenium (IV) oxide were purchased from Strem Chemicals, Inc. 7-Dehydrocholesterol (>98%), 2,4-dinitrophenyl-hydrazine (>99%), *p*-toluenesulfonyl hydrazide (97%), *tert*-butyl hydroperoxide solution (~5.5 M in decane) and all other chemical reagents at the highest grade were purchased from Sigma-Aldrich Co. and were used without further purification. Hexanes, ethyl acetate, methylene chloride, and methanol (all 99.9%) were purchased from Thermo Fisher Scientific, Inc.

Cell cultures and treatment of HFs and Neuro2a cells with epoxide 1 and triol 2

Neuroblastoma cell line Neuro2a was purchased from the American Type Culture Collection (Rockville, MD). Control (GM05758 and GM05565) and SLOS (GM05788 and GM03044) HFs were purchased from the Corriell Institute. The use of repository human cell lines from Corriell Institute is exempted from Institutional Review Board review.

Dhcr7-deficient and nonsilencing Neuro2a cells were generated as described previously (27). All cell lines were maintained in DMEM supplemented with L-glutamine, 10% FBS (Thermo Scientific HyClone, Logan, UT), and penicillin/streptomycin at 37°C and 5% CO_2. For *Dhcr7*-deficient Neuro2a cells and SLOS HF, cells were cultured with medium containing 10% Chol-deficient serum (Thermo Scientific HyClone Lipid Reduced FBS). To determine the levels of Chol, 7-DHC, and **DHCEO** in different cell lines (Table 1), cells were cultured in medium containing 10% Chol-deficient serum (Thermo Scientific HyClone Lipid Reduced FBS) for 5 days. This medium did not contain a detectable level of Chol. The cell pellet was collected by centrifugation at 250 *g* for 5 min at +4°C and washed with PBS buffer. The medium and PBS were discarded and the cell pellet was lysed with NP 40 lysis buffer [50 mM Tris, pH 7.2, 150 mM NaCl, 5 mM EDTA, 0.5% NP-40, 0.5% sodium deoxycholate, protease inhibitor mixture (Sigma), phoshatase inhibitor mixture (Sigma), and 100 mM phenylmethylsulfonyl fluoride] and the protein concentration was determined using Protein D_c photometric assay (Bio-Rad). The cell lysate was frozen at −80°C until lipid extraction and oxysterol separation (vide infra).

For the treatment of epoxide **1** and triol **2**, all HF and Neuro2a cell lines were expanded and maintained in DMEM media supplemented with 10% FBS in the same way as described above. Lipid-deficient FBS was not used in these experiments. To perform the experiments, the HF cells were plated at a density of 5.0×10^5 cells in 60 mm cell culture dishes (Sarstedt) and the Neuro2a cells were plated at a density of ca. 1×10^6 cells in 100 mm dishes. Both cell lines were allowed 12 h to attach to the dishes. Both were then cultured in media enriched with 5 μM of either **1** or **2** (n = 3) for 24 h. After 24 h in cell culture incubator, both cell culture medium and cells were harvested. Medium was collected, frozen on dry ice, and transferred to −80°C storage. The cells were collected in the same way as above, as well as the determination of the protein concentration. The cell lysate and the medium were frozen at −80°C until lipid extraction and oxysterol separation (vide infra).

Dhcr7-KO mice

Dhcr7-KO (*Dhcr7*$^{tm1Gst/J}$) mice were purchased from Jackson Laboratories (catalog # 007453). The mice were kept and bred in Division of Animal Care facilities at Vanderbilt University. Embryos at embryonic day 20 (E20) were dissected from pregnant females and the tail was removed from each embryo for genotyping. The genomic DNA from mouse tails was extracted using REDExtract-N-Amp Tissue PCR kit (Sigma-Aldrich). The primers used for PCR were: forward: ggatcttctgagggcagcctt, reverse: tctgaacccttggctgatca, neo: ctagaccgcggctagagaat. Embryonic heads were removed and brains were rapidly dissected and instantly frozen in precooled 2-methylbutane (on dry ice) and stored at −80°C until lipid extraction. All procedures were performed in accordance with the Guide for the Humane Use and Care of Laboratory Animals. The use of mice in this study was approved by the Institutional Animal Care and Use Committee of Vanderbilt University.

Lipid extraction, separation, and HPLC-APCI-MS/MS analyses

An appropriate amount of d_7-**DHCEO** standard was added to each sample before sample processing. Mouse brain tissues were homogenized in Folch solution (5 ml, chloroform/methanol = 2/1, containing 0.001M butylated hydroxytoluene and

PPh_3) by blade homogenizer. The resulting mixture was left under Ar at room temperature for 30 min. Cell lysates were extracted directly with the same Folch solution. NaCl aqueous solution (0.9%, 1 ml) was then added and the resulting mixture was vortexed for 1 min and centrifuged for 5 min. The lower organic phase was recovered, dried under nitrogen, redissolved in methylene chloride, and subjected to separation with NH_2-SPE [500 mg; the column was conditioned with 4 ml of hexanes and the neutral lipids containing oxysterols were eluted with 4 ml of chloroform/2-propanol (2/1)]. The eluted fractions were then dried under nitrogen and reconstituted in methylene chloride (400 μl) for HPLC-atmospheric pressure chemical ionization (APCI)-MS/MS analyses. The analyses were carried out similarly to the method described previously (12, 27). HPLC conditions: Silica 4.6 mm × 25 cm column; 5μ; 1.0 ml/min; elution solvent: 10% 2-propanol in hexanes. For MS, selective reaction monitoring (SRM) was employed to monitor the dehydration process of the ion $[M+H]^+$ or $[M+H-H_2O]^+$ in the MS. Thus, for oxysterols with molecular weight of [7-DHC+2O], dehydration from *m/z* 417 to 399 and from *m/z* 399 to 381 were monitored. For [7-DHC+3O], *m/z* 415 to 397 was monitored. In this way, masses that correspond to 7-DHC plus 1, 2, 3, and 4 oxygen atoms can be monitored. The parent ion of each chromatogram was marked in the corresponding panel. For example, the $[7\text{-DHC+2O+H}^+\text{-H}_2\text{O}]$ panel suggests SRM of $[7\text{-DHC+2O+H}^+\text{-H}_2\text{O}]$ to $[7\text{-DHC+2O+H}^+\text{-2H}_2\text{O}]$ (*m/z* 399 to *m/z* 381) in the mass spectrometer. For quantification of 7-DHC and Chol, dehydration ions $[7\text{-DHC+H}^+\text{-H}_2\text{O}]$ and $[\text{Chol+H}^+\text{-H}_2\text{O}]$ were monitored at *m/z* 367 and 369, respectively. The deuterated version of each compound was monitored in a similar way but with a difference of *m/z* = 7.

RP-HPLC-ESI-MS/MS analysis of 2,4-DNPH derivatives of cell and tissue extracts

Cells or tissues were worked up as described above and thus obtained sample solutions were blown dry under a stream of nitrogen. The residues were incubated in 500 μl 2,4-DNPH saturated solution in methanol and 50 μl 1N HCl at room temperature for 12 h. The resulting solution was analyzed by reverse phase (RP) HPLC-ESI-MS/MS. HPLC condition: 150 × 2 mm Phenomenex C18 column; 3μ; 0.2 ml/min; elution solvent, acetonitrile/methanol = 70/30. MS condition: spray voltage, 4,500 V; sheath gas, 60 mTorr; sweep gas, 8 mTorr; aux gas, 55 mTorr; tube lens, 240 V; skimmer offset, 28 V; collision pressure, 1.4 mTorr; collision energy, 10 V. d_0- and d_7-**DHCEO**-DNPH standards were prepared and analyzed in a similar way. d_0-**DHCEO**-DNPH was isolated by HPLC-ultraviolet (UV) using the same HPLC condition and the structure was confirmed by NMR and MS. ^{1}H NMR of d_0-**DHCEO**-DNPH (600 MHz, $CDCl_3$): δ 0.63 (s, 3H), 0.87 (d, 3H, *J* = 2.7 Hz), 0.88 (d, 3H, *J* = 2.7 Hz), 0.89 (s, 3H), 0.95 (d, 3H, *J* = 6.4 Hz), 1.58-1.68 (m, 3H), 1.70-1.81 (m, 3H), 1.92 (br d, 1H, *J* = 9.9 Hz), 1.99 (m, 1H), 2.01 (dd, 1H, *J* = 13.6, 11.6 Hz), 2.17 (m, 2H), 2.41 (m, 2H), 4.14 (m, 1H), 6.00 (br s, 1H), 7.99 (d, 1H, *J* = 9.6 Hz), 8.31 (dd, 1H, *J* = 9.6, 2.5 Hz), 9.14 (d, 1H, *J* = 2.5 Hz), 11.4 (s, 1H, NH). ^{13}C NMR of d_0-**DHCEO**-DNPH (150 MHz, $CDCl_3$): δ 12.6, 17.4, 18.9, 22.1, 22.68, 22.70, 23.0, 24.0, 27.9, 28.2, 30.6, 30.8, 36.1, 38.3, 39.2, 39.6, 40.2, 45.1, 45.3, 56.1, 56.4, 67.9, 76.9, 106.8, 116.6, 123.7, 129.5, 130.2, 138.1, 145.2, 154.4, 159.5.

Syntheses

See the supplementary data for the syntheses of d_7-7-DHC, d_0- and d_7-**DHCEO**, 5α,6α-epoxycholest-7-en-3β-ol (**1**) and 7-cholesten-3β,5α,6β-triol (**2**).

RESULTS

Oxysterol profiles of human SLOS fibroblasts and *Dhcr7*-deficient Neuro2a cells

Fibroblasts derived from human skin are used as cellular models to study the pathophysiology of a variety of disorders (28–31), especially those involved in lipid metabolism (32–34). For example, fibroblasts from SLOS patients contain elevated levels of 7-DHC and these cells have been used to establish methods for 7-DHC analysis and to determine the biological effects of this lipid (32, 33). It has been suggested by others that SLOS patients are subject to oxidative stress and may have elevated oxysterol levels (35–37). Based on our studies showing the extreme reactivity of 7-DHC toward free radical chain oxidation in solution (11), we reasoned that elevated levels of 7-DHC oxysterols would be formed in HFs from SLOS patients. To test this hypothesis, fibroblasts from two SLOS patients and those from two matched healthy donors were grown and our previously reported HPLC-MS method was employed to analyze the oxysterol profile in these fibroblasts (12). Briefly, all fibroblasts were grown for 5 days in lipid-deficient serum and collected for lipid extraction, separation, and normal phase (NP) HPLC-MS analysis (see Materials and Methods). Lipid-deficient serum, instead of regular FBS, is necessary for the cells to start their own Chol biosynthesis, which leads to the build-up of 7-DHC in SLOS samples.

Representative HPLC-MS chromatograms of control and SLOS HFs are shown in **Fig. 1A** (Control) and Fig. 1B (SLOS). Several new peaks that have *m/z*s corresponding to 7-DHC oxysterols are observed in all of the SLOS HF chromatograms compared with those of the corresponding controls. It is of note that the oxysterol profile of SLOS HF is only slightly different from the profile we observe in *Dhcr7*-deficient Neuro2a cells (27). Whereas the compound eluting at 9 min is a major one in *Dhcr7*-deficient Neuro2a cells, it is the predominant one in the SLOS HFs. Four minor peaks in the $[7\text{-DHC+2O+H}^+\text{-H}_2\text{O}]$ and $[7\text{-DHC+3O+H}^+\text{-H}_2\text{O}]$ panels that were observable in *Dhcr7*-deficient Neuro2a cells are not detected in SLOS HFs (27).

Oxysterol profiles of *Dhcr7*-KO mouse brain

The *Dhcr7*-KO mice were generated to characterize the pathophysiology and neurophysiology underlying SLOS and to provide a model system for testing therapeutic interventions (3, 38). The KO mouse is featured by a predominant amount of 7-DHC over Chol, an extreme case of SLOS. Typically, in surviving SLOS patients, Chol is still the major sterol compared with 7-DHC and 8-DHC (39). Physical abnormalities found in newborn KO mice also have their counterparts in affected children (3, 38). The mouse model has been used to explore the mechanisms by which 7-DHC inhibits sterol biosynthesis (3), sterol metabolism of embryonic mice (40), neuroanatomical defects (41), and signaling in the nervous system (42).

Therefore, in the current study we used *Dhcr7*-KO mice to examine the 7-DHC oxysterol profile in vivo, specifically

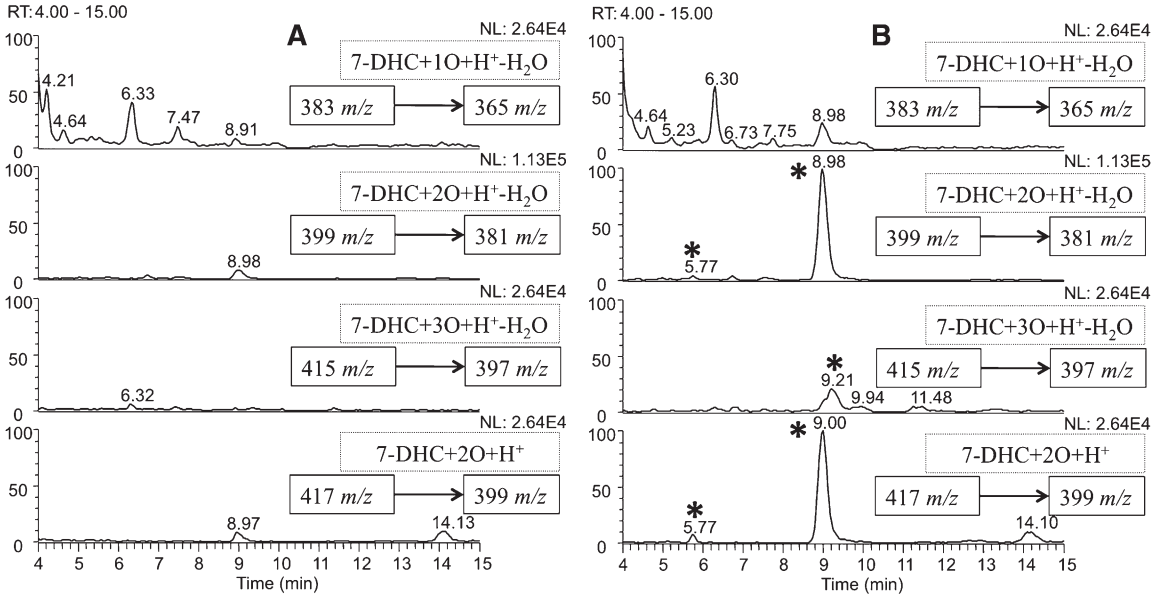

Fig. 1. NP-HPLC-APCI-MS-MS (Silica 4.6 mm × 25 cm column; 5μ; 1.0 ml/min; elution solvent: 10% 2-propanol in hexanes) chromatograms of the oxysterols from (A) control HFs and (B) SLOS HFs after being incubated in DMEM with lipid-deficient serum for 5 days. New peaks in B relative to control are marked with *.

in brain tissue. The brain has a very high content of Chol (43, 44) and it is known that the brain starts its own independent Chol biosynthesis at approximately E12 (40). *Dhcr7*-KO mice accumulate 7-DHC and a high level was reported in the brain at postnatal day 0. Because these KO mice die shortly after birth, we took brain tissue for analysis at late embryonic stages (E20). Representative NP-HPLC-MS chromatograms of the isolated sterol mixture from brain are shown in **Fig. 2A** wild type (WT), 2B (KO), and supplementary Fig. I (heterozygous, Het).

Similar to the data obtained in cultured human SLOS fibroblasts, multiple new peaks that correspond to the *m/z*s of 7-DHC oxysterols were observed in the chromatograms of *Dhcr7*-KO mouse brains when compared with their corresponding controls and Hets. The peak at RT = 9 min was again observed as a major oxysterol in the *Dhcr7*-KO sample.

We tentatively assigned the 9 min peak as **DHCEO**, (**Fig. 3**) one of the oxysterols previously isolated from 7-DHC free radical oxidation (12). The structure assignment was based on an identical mass spectrum and retention time when compared with a standard isolated from 7-DHC oxidation in solution and from an independent synthesis of the compound (see supplementary Fig. II) (12). We reported the tentative assignment of this peak in *Dhcr7*-deficient Neuro2a cells in our previous publication (27). In the current study, we provide multiple lines of evidence to support our assignment in both cell and mouse models for SLOS, making use of a synthetic deuterated standard as described below.

Preparation of [25,26,26,26,27,27,27-d$_7$]standards

The mass spectrum of **DHCEO** provides a molecular ion and fragments of loss of one or multiple water molecules but it is otherwise uninformative. In fact, oxysterols isolated from the product mixture of 7-DHC solution oxidation all gave multiple loss-of-water ions in the mass spectrometer and some of these oxysterols gave fragments with the same *m/z* values as those of **DHCEO** (12). To fully elucidate the structure of the 9 min peak, we prepared an authentic deuterated standard of **DHCEO** and compared different chemical derivatives of the cell or tissue extracts with those of the deuterated standard. Thus, [25,26,26,26,27,27,27-d_7]7-dehydrocholesterol acetate was prepared from the corresponding d_7-Chol acetate following known procedures (see supplementary data) (45, 46). The resulting d_7-7-DHC acetate was then converted to d_7-7-DHC by $LiAlH_4$ reduction and to d_7-**DHCEO** by oxidation of the C5 = C6 double bond with RuO_4 followed by hydrolysis under basic conditions (see supplementary data) (47). An appropriate amount of the d_7-**DHCEO** standard was added to each cell or tissue extract before preparing the samples for NP-HPLC-MS analysis. The resulting HPLC-MS chromatograms show that the 9 min peak coelutes with the d_7-standard and has the same MS pattern, differing only by the mass of the seven deuterium atoms (Fig. 3).

Characterization of DHCEO in cells and tissues

In addition to the evidence that the 9 min peak coelutes with d_7-**DHCEO** on an NP HPLC column, functional group derivatization was employed to support the notion that **DHCEO** is present in cells and tissues. 1,4-Dinitrophenyl hydrazine (DNPH) has been frequently used to derivatize carbonyl groups, such as ketones and aldehydes, in HPLC-MS studies (48, 49). Standard DNPH adducts of **DHCEO** were prepared by incubating the corresponding d_0- and d_7-**DHCEO** with DNPH in methanol under acidic conditions at room temperature over 12 h (see Materials and Methods). The d_0-adduct was purified by RP HPLC-UV and its

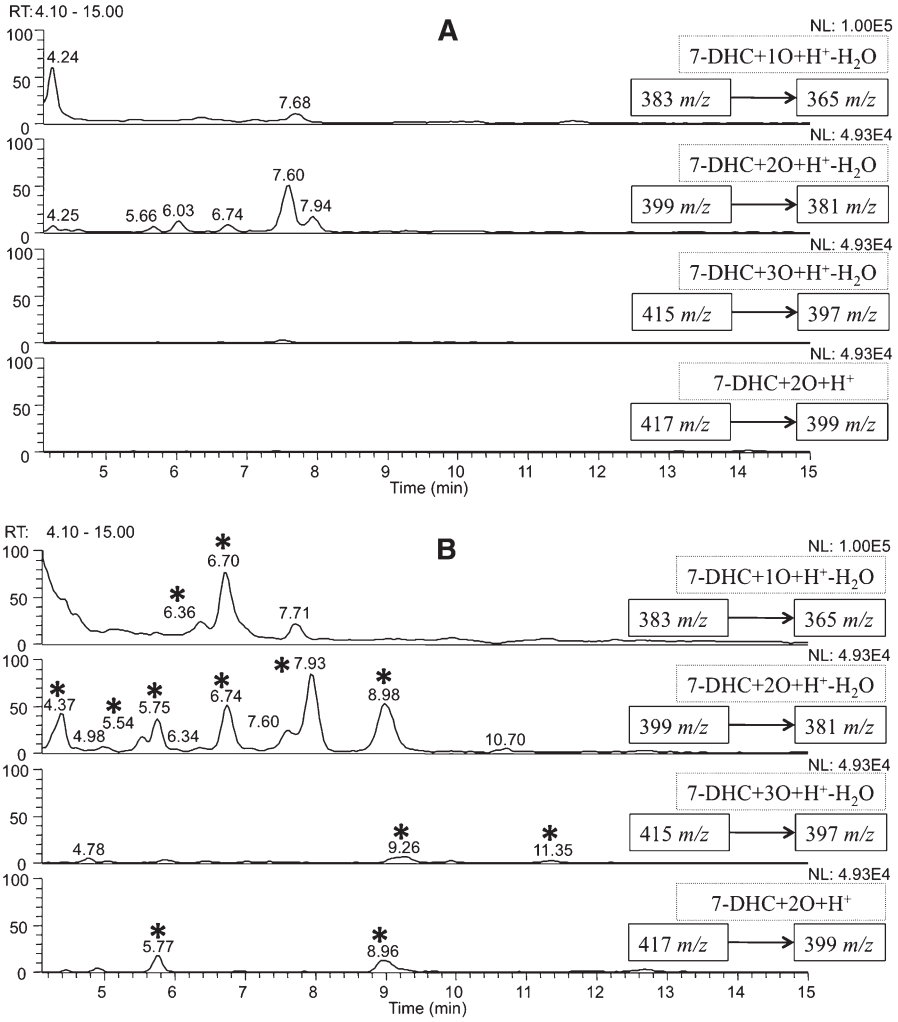

Fig. 2. NP-HPLC-APCI-MS-MS chromatograms of the oxysterols from (A) WT E20 mouse brain and (B) *Dhcr7*-KO E20 mouse brain. New peaks in B relative to control are marked with *.

identification was confirmed by NMR and ESI-MS (ESI, instead of APCI, is the better ionization source for the DNPH adduct; see **Fig. 4** and Materials and Methods section).

Loss-of-water from the molecular ion of **DHCEO**-DNPH was chosen for SRM in the RP-HPLC-ESI-MS analysis. As shown in **Fig. 5A**, the retention time of the d_0-adduct is ~ 0.1 min longer than that of the d_7-adduct. Samples of SLOS HF and *Dhcr7*-KO mouse brain (along with control HF and WT mouse brain) were mixed with **DHCEO** d_7-standard and the mixture was converted to the DNPH adducts by the standard protocol and RP-HPLC-MS analyses confirmed the presence of d_0-**DHCEO** in each SLOS sample (Fig. 5B, C).

In a similar way, picolinoyl derivatization followed by HPLC-MS analysis and TMS derivatization followed by GC-MS verified the presence of **DHCEO** in *Dhcr7*-deficient Neuro2a cells (see supplementary Figs. III and IV) (50, 51). The TMS procedure also confirms the presence of two free hydroxyl groups in the compound.

Quantification of Chol, 7-DHC, and DHCEO in cells and tissues

To quantify **DHCEO** in cells and tissues, a known amount of d_7-**DHCEO** was added to each cell lysate or tissue before lipid extraction and the sample was worked up for HPLC-MS analysis by our standard protocol (see Materials and Methods). Endogenous **DHCEO** in each sample was calculated by comparison of the HPLC-MS response of d_0-**DHCEO** to that of the internal d_7-standard. The results are summarized in **Table 1**. The levels of 7-DHC and Chol were also determined with the use of d_7-7-DHC and d_7-Chol as external standards by a similar HPLC-MS method, monitoring the loss-of-water ion from each sterol by selective ion monitoring in the HPLC-MS (see Materials and Methods and supplementary Fig. V). Note that each sample was diluted 30 to 50 times for 7-DHC and Chol quantification to bring the sample to an appropriate concentration range for HPLC-MS analysis. The calculated 7-DHC/Chol ratios are also summarized in Table 1. Due to analytical limitations of our standard procedure, the level of 7-DHC could not be accurately determined when the 7-DHC/Chol ratio was less than 0.01 (see Table 1 and supplementary Fig. V).

As seen in Table 1, the level of **DHCEO** found in each SLOS model sample was significantly higher than in the corresponding control, a result that parallels the levels of 7-DHC in the samples. Indeed, there was a strong and

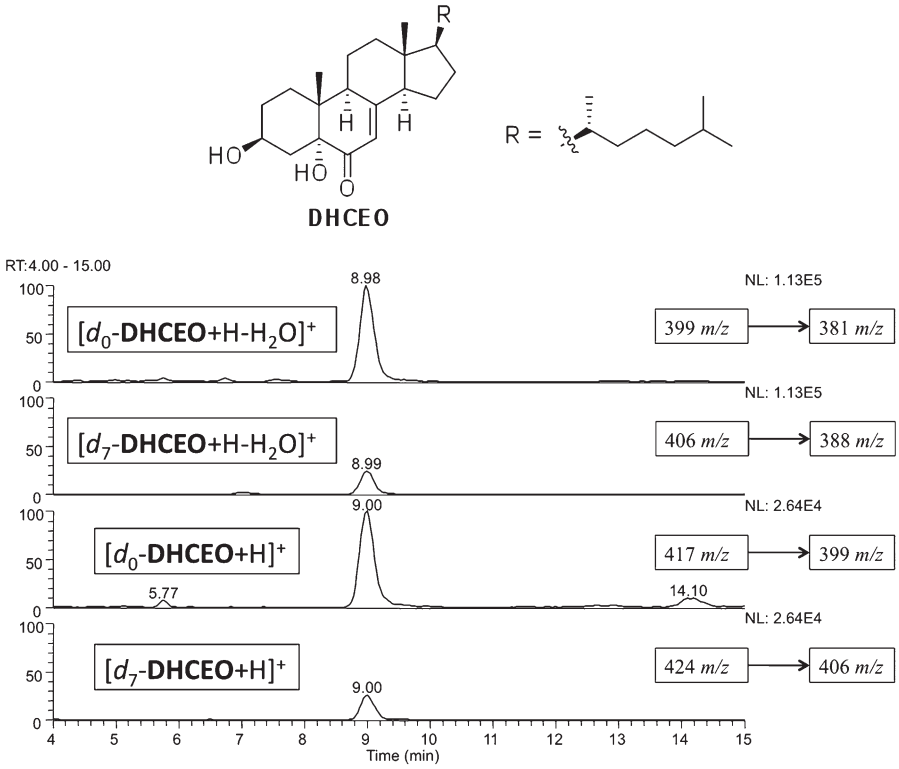

Fig. 3. Structure of a major oxysterol, 3β,5α-dihydroxycholest-7-en-6-one (**DHCEO**) and NP-HPLC-MS-MS chromatogram of **DHCEO** in the presence of d_7-**DHCEO** standard from SLOS HF after being incubated in DMEM with lipid-deficient serum for 5 days.

significant correlation between the levels of 7-DHC and **DHCEO** in all samples where **DHCEO** was observed (R = 0.9851). It is of some interest that **DHCEO** was observed at high levels even in the control HFs that were cultured in the presence of lipid-deficient serum.

DHCEO can be formed from 5α,6α-epoxycholest-7-en-3β-ol (1) and 7-cholesten-3β,5α,6β-triol (2) in HFs and Neuro2a cells

We propose that **DHCEO** can be formed from 7-DHC by a mechanism similar to that suggested for formation of the analogous oxysterol, cholestan-6-oxo-3β,5α-diol (also named as 3β,5α-dihydroxy-cholestan-6-one, **DHCAO**), from Chol (**Fig. 6**) (12). The proposed mechanism for **DHCAO** formation proceeds via the 5,6-epoxide by a free radical or enzymatic process followed by ring-opening of the epoxide by a hydrolase and secondary alcohol oxidation (52–58). To test this proposal for **DHCEO** formation, 7-DHC 5α,6α-epoxide (**1**) was prepared by epoxidation of 7-DHC with peroxyimidic acid generated in situ from acetonitrile and hydrogen peroxide under basic condition (see supplementary data) (59). The 3β,5α,6β-triol (**2**) was prepared by hydrolysis of **1** in acidic buffer (see supplementary data) (60).

With the newly synthesized 7-DHC 5α,6α-epoxide (**1**) standard in hand, we were able to identify it as one of the major products formed from free radical oxidation of 7-DHC. An unidentified peak at retention time 5.45 min in our previously published chromatogram of a 7-DHC free radical oxidation mixture was confirmed to be epoxide **1** (see supplementary Fig. VI) (12). A subsequent free radical oxidation of 7-DHC following the previously published procedure further verified the presence of epoxide **1** as a major product (12). This epoxide is apparently not stable enough to survive column chromatography on silica gel during product isolation, which is the likely reason that it was not found in our earlier studies. It is well known in the literature that epoxides can be formed from alkenes through peroxyl radical addition (61, 62) such as the formation of Chol epoxides (57, 58).

Compounds **1** or **2** (5 μM) were incubated in culture medium in the absence of any cells (blank medium), with control Neuro2a cells, and with control or SLOS HFs. The cell experiments were carried out in DMEM supplemented with 10% FBS instead of lipid-deficient serum. At the end of each experiment, both cell pellets and the medium were collected and levels of **DHCEO** were measured in both, the sum of which gave a total level of **DHCEO** in each experiment. Determination of the total level of **DHCEO** is necessary because the exchange of this oxysterol between the medium and the cells could occur (vide infra). No **DHCEO** was observed in any sample in the absence of compound **1** or **2** (see **Fig. 7A** for a representative chromatogram). The incubation of either epoxide **1** or triol **2** for 24 h in the same medium gave a significant amount of **DHCEO** in all samples including the experiments carried out in the blank medium (Fig. 7B, supplementary Figs. VII–IX, and **Table 2**). The experiments in blank medium show that epoxide **1** and triol **2** can form **DHCEO** spontaneously under the incubation conditions,

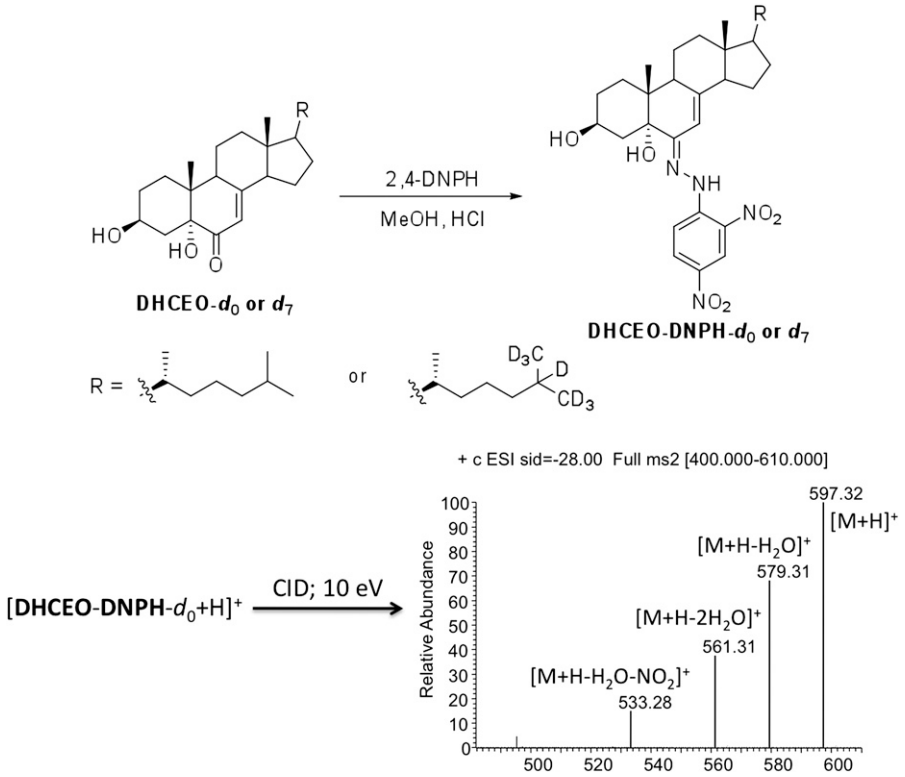

Fig. 4. Derivatization of d_0- or d_7-**DHCEO** with 1,4-dinitrophenyl hydrazine (DNPH) and the collision-induced dissociation (CID) mass spectrum of the d_0-adduct molecular ion in ESI-MS analysis.

confirming the nonenzymatic mechanism shown in Fig. 6. The levels of **DHCEO** formed from triol **2** are 4 to 12 times higher than levels generated from epoxide **1** both in fibroblast cell lines and in the blank medium whereas Neuro2a cells generate about the same levels of **DHCEO** from both precursors (**Table 3**). The total levels of **DHCEO** formed in cells is much higher than the levels in plain medium or medium with serum, suggesting that biological processes in the cells promote the transformation of compounds **1** and **2** to **DHCEO**. When levels of **DHCEO** were normalized to protein weight, Neuro2a cells appear to convert the epoxide and triol more efficiently to **DHCEO** (Table 3). In addition, a different distribution ratio of **DHCEO** in cells and the medium was observed in different cell lines (Table 3). Metabolism of these oxysterols is likely to be cell specific and the differences between the incubation outcomes of **1** and **2** in fibroblasts and Neuro2a cells is likely the result of differential metabolism.

Antioxidant reduces the levels of DHCEO in SLOS HFs

Because **DHCEO** and associated oxysterols are toxic to Neuro2a cells, we have initiated efforts to reduce the levels of these compounds in cultured cells, specifically in SLOS HF. Mechanisms for the formation of **DHCEO** from 7-DHC could involve both free radical chain oxidation and cytochrome P450-catalyzed conversion and for this reason, preliminary experiments exploring the effect of antioxidants on **DHCEO** formation were initiated. Pyridinol and pyrimidinol antioxidants, such as antioxidant **3**, show better properties than α-tocopherol and other antioxidants in chemical tests and in studies of neuronal oxidative stress (63–66), and experiments were therefore carried out with SLOS HFs to assess the potential of these antioxidants to reduce the levels of oxysterols. SLOS fibroblasts in lipid-deficient serum were incubated for 5 days in the absence or presence of 10 μM antioxidant **3** (**Fig. 8**), and the level of **DHCEO**, the major oxysterol in fibroblasts, was quantified by HPLC-MS-MS using the d_7-**DHCEO** standard as described (Fig. 8). As shown in Fig. 8, antioxidant **3** reduced the level of **DHCEO** significantly (by ca. 55%, $P < 0.005$) in treated SLOS fibroblasts compared with untreated SLOS HF, whereas the 7-DHC/Chol ratios were not affected significantly.

DISCUSSION

Given similar biological environments, concentrations, and rates of initiation, the free radical oxidation of 7-DHC will generate some 200 times more oxysterols than will be formed from Chol, based on experimentally measured propagation rate constants for the two sterols. In addition, 7-DHC gives a much more complex mixture of oxysterols than does Chol. The complexity of the 7-DHC oxysterol product profile comes from the multiple reactive sites available for hydrogen atom abstraction, such as H-9 and H-14, and the multiple mechanistic options provided by the conjugated diene in ring B of the sterol (12).

The complex free radical oxidation mechanism of 7-DHC leads to oxysterols having the molecular weight of 7-DHC plus up to three oxygen atoms and these primary products include cyclic peroxides, epoxides, and tetraols

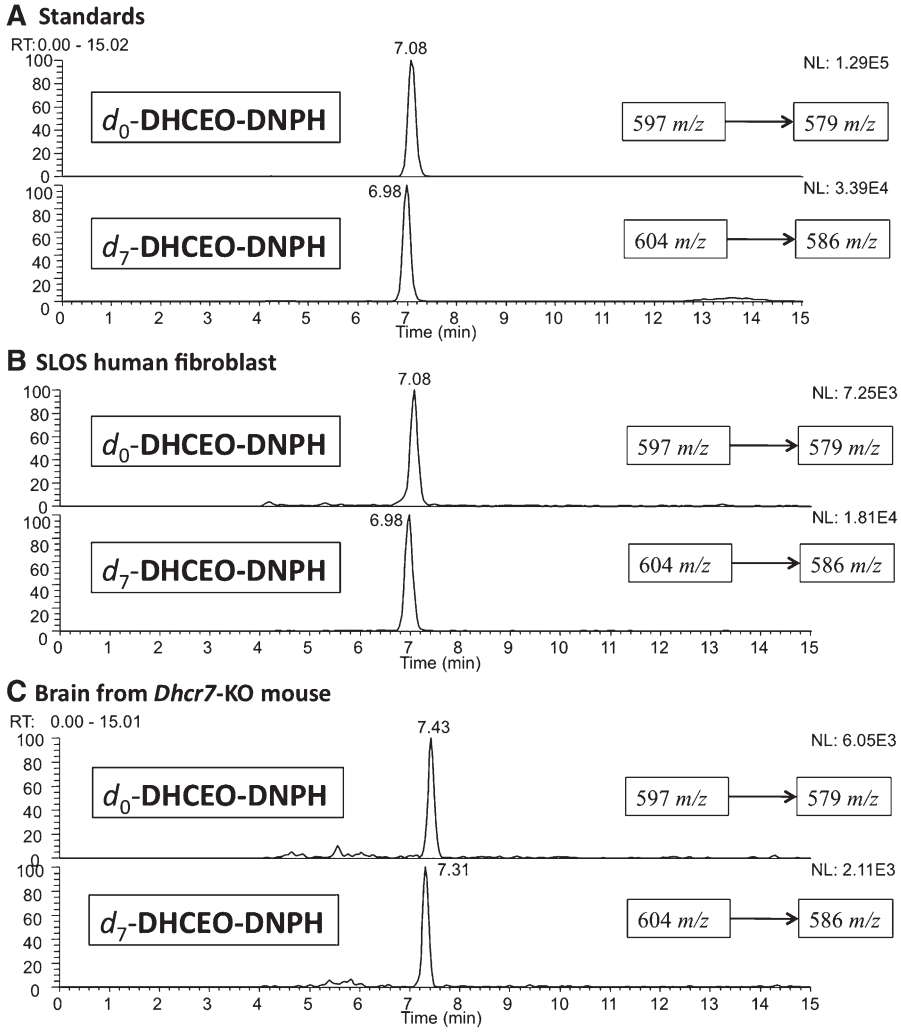

Fig. 5. RP-HPLC-ESI-MS-MS (150 × 2 mm C18 column; 3μ; 0.2 ml/min; elution solvent: acetonitrile/methanol = 70/30) chromatogram on the DNPH adducts of (A) d_0- and d_7-**DHCEO** standards, (B) SLOS HF in the presence of internal d_7-**DHCEO** standard, and (C) E20 *Dhcr7*-KO mouse brain in the presence of internal d_7-**DHCEO** standard. The SLOS samples were incubated in DMEM with lipid-deficient serum for 5 days.

(12). Analysis of 7-DHC-derived oxysterols in HFs from SLOS individuals and the brain tissues from the *Dhcr7*-KO mouse model of SLOS shows a profile of oxysterols having up to three additional oxygen atoms relative to the parent structure (Figs. 1B, 2B). Oxysterols with molecular weight of [7-DHC+2O] constitute the majority of the oxysterols observed in these SLOS models, **DHCEO** being one of them, but compounds with 7-DHC plus one or three oxygen atoms are also observed. **DHCEO** was indeed isolated as a minor product in the free radical oxidation of 7-DHC (12), but the oxysterol profiles in SLOS HFs and *Dhcr7*-KO mouse brain are quite different from the product profile of 7-DHC free radical oxidation in solution. Indeed, differences in the product profiles were observed from the

TABLE 1. **DHCEO** and sterol concentrations in Neuro2a cells, HFs, and brains from mice at embryonic day 20

	Neuro2a		Human fibroblast		E20 mouse brain		
	Control	Dhcr7-def	Control	SLOS	WT	Het	KO
DHCEO (ng/mg)	0	3.51 ± 0.08[a]	39.5 ± 8.5	333 ± 115[a]	0.014 ± 0.004	0.039 ± 0.013[b]	1.45 ± 0.16[a]
7-DHC (μg/mg)	–	3.09 ± 0.02[a]	2.05 ± 0.43	19.1 ± 1.3[a]	–	–	3.21 ± 0.33[a]
Chol (μg/mg)	34.6 ± 5.5	34.4 ± 8.4	108 ± 21	65 ± 10[c]	3.12 ± 0.60	2.97 ± 0.12	0.42 ± 0.07[a]
7-DHC/Chol	–	0.093 ± 0.022[a]	0.019 ± 0.002	0.30 ± 0.04[a]	–	–	7.76 ± 0.72[a]

Per mg of protein for Neuro2a and HF; per mg of tissue for mouse brain (wet weight); statistical analyses are all relative to Control or WT; n = 3 for all Neuro2a and mouse samples; n = 6 for HF (triplicate of two different cell lines for control or SLOS, see Materials and Methods). –, Not available due to analytical limitation; WT, wild-type; Het, $Dhcr7^{+/-}$; KO, $Dhcr7^{-/-}$.

[a] $p < 0.0005$.

[b] $p < 0.05$.

[c] $p < 0.005$.

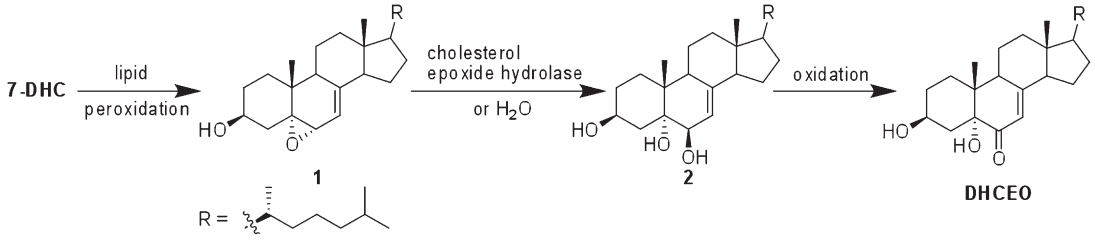

Fig. 6. Proposed formation mechanism of **DHCEO**.

different SLOS models, a result that is perhaps not surprising because metabolism will likely vary in different cells and tissue models. Cytochrome P450 oxidation, for example, is one important metabolic pathway that sterols undergo, and it is quite likely that P450 secondary oxidation reactions could alter the structure of the primary oxidative stress products formed from 7-DHC. Enzymatic oxidation of 7-DHC itself is known (67), but these enzymatically-derived oxysterols typically have one additional oxygen atom relative to the corresponding sterol. The product profile found in the *Dhcr7*-KO mouse brain does indeed include two oxysterols having a mass of [7-DHC+1O] and experiments are ongoing to identify these compounds.

Taking data from all the experiments together, there is an excellent correlation between the levels of **DHCEO** determined and the measured levels for 7-DHC ($R = 0.9851$), suggesting that **DHCEO** is derived from 7-DHC and can be used as a biomarker for 7-DHC oxidation. **DHCEO** is an especially prominent product in SLOS HF and it is even present at high levels in control HF cells, indicating a Chol biosynthesis pathway quite different from Neuro2a cells (Table 1). Indeed, HFs are slow-growing primary cells whereas Neuro2a cells are a fast-dividing tumor cell line. 7-DHC is present at high concentrations in human skin where it serves as a precursor to previtamin D_3 upon UV irradiation (68). It is worth noting that although there is a good correlation between the levels of **DHCEO** and 7-DHC, the amount of **DHCEO** formed per unit of 7-DHC varies in different system. For example, in either control or SLOS HF, the level of **DHCEO** is ~2% that of 7-DHC whereas in *Dhcr7*-deficient Neuro2a cells, the value is 0.1% and in *Dhcr7*-KO mouse brain, the value is 0.05%. The variability in **DHCEO**/7-DHC ratios may indicate different metabolism and/or different antioxidant capacity in different systems.

The observation of **DHCEO** as one of the major oxysterols in all SLOS cells and tissues examined suggests that there may be a common mechanism for its formation. Incubation of blank medium or different cell lines with 7-DHC 5α,6α-epoxide **1** or 3β,5α,6β-triol **2** produces **DHCEO**, which provides evidence that compounds **1** and **2** are viable intermediates in the transformation of 7-DHC to **DHCEO** (see Fig. 6). More importantly, biological processes in the cells apparently accelerate the metabolism of epoxide **1** and triol **2** to **DHCEO**.

A free radical mechanism for formation of **DHCEO** via an intermediate epoxide had been previously suggested (12) and 7-DHC 5α,6α-epoxide **1** was found to be a major free radical oxidation product of 7-DHC in the current study. Although this lends credence to the free radical

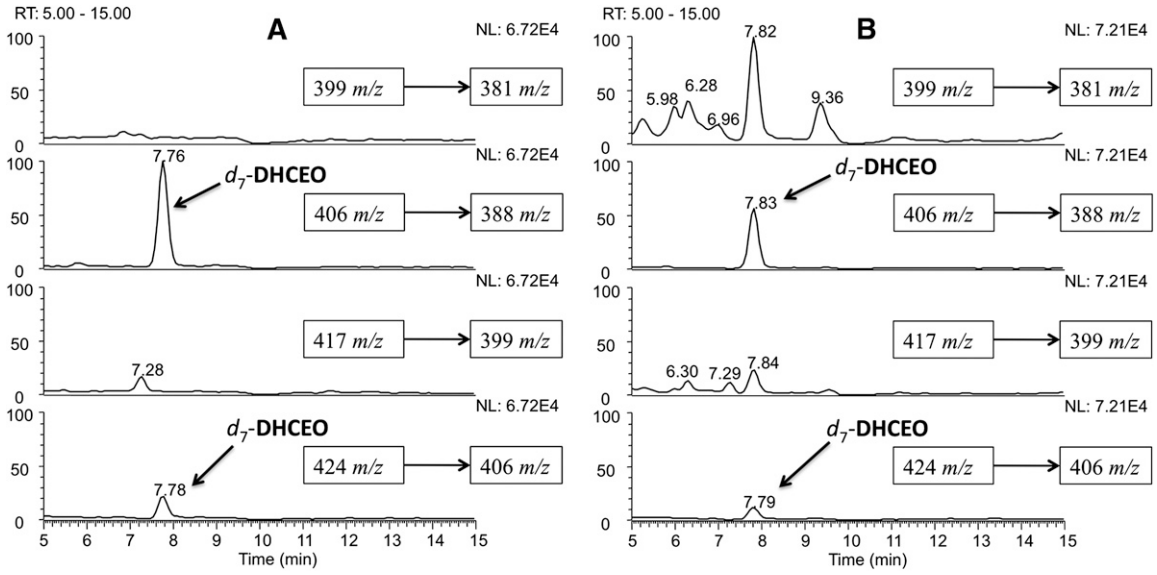

Fig. 7. NP-HPLC-APCI-MS-MS chromatograms of oxysterols from control HFs in DMEM media supplemented with 10% FBS (A) under control condition, and (B) after incubating with 5 μM of 5α,6α-epoxycholest-7-en-3β-ol (**1**) for 24 h. d_7-**DHCEO** was added when preparing the samples for HPLC-MS analysis to indicate the presence or absence of native d_0-**DHCEO** and to quantify it.

TABLE 2. Total levels of **DHCEO** formed from 5 μM **1** (epoxide) or **2** (triol) in culturing medium or in the presence of different cell lines over 24 h

	No **1** or **2**	DMEM	DMEM+serum	HF-control	HF-SLOS	Neuro2a-control
DHCEO from **1** (ng)	0	33 ± 3	36 ± 5	162 ± 5[a]	127 ± 10[a]	2233 ± 180[a]
DHCEO from **2** (ng)	0	340 ± 32	445 ± 70	676 ± 63[b]	590 ± 31[b]	1833 ± 75[a]

Regular FBS was used here; statistical analyses were performed against DMEM+serum experiments.
[a] $p < 0.0005$.
[b] $p < 0.05$.

mechanism, we cannot exclude possible enzyme involvement in the initial epoxide formation. There is indeed some evidence that the 5α,6α- and/or 5β,6β-epoxy sterols can be formed enzymatically from Chol in bovine liver microsomes and adrenal cortex (55, 56), but no specific enzyme has been shown to catalyze the epoxidation of Chol. It is also known that Chol epoxides are formed nonenzymatically from peroxyl radicals under lipid peroxidation conditions (57, 58) and it seems likely that 7-DHC, a conjugated diene, will be even more prone to undergo peroxyl radical attack than Chol. The evidence suggests then, that free radical conversion of 7-DHC to the epoxide does occur, but it leaves open the question as to whether an enzymatic pathway also exists for this transformation. These and other mechanistic questions that arise for **DHCEO** formation in cells and tissue are under active investigation and the results of these studies will be reported in due course.

Oxidation products formed from lipid peroxidation can be biomarkers of oxidative stress, but they can also exert various biological activities, oxysterols being notable examples. Oxysterols are important regulators of Chol homeostasis by binding liver X receptors or other nuclear receptors and by suppressing the sterol regulatory element binding protein pathway (26). Oxysterols and Chol biosynthetic intermediates such as lanosterol are reported to stimulate degradation of HMG-CoA reductase by binding to Insigs (69). Interestingly, 7-DHC is also reported to suppress sterol biosynthesis by inducing proteolysis of HMG-CoA reductase (3). This observation of activity may be partially a result of oxysterols that are generated from 7-DHC oxidation during the incubation time of the experiments. Indeed, the extreme oxidizability of 7-DHC raises the possibility of contamination by 7-DHC oxysterols in any experiment carried out with this sterol. As a normal precaution, 7-DHC should be freed of oxysterol contaminants before any experiments to assess its biological activity in any assay.

In vitro tests on **DHCEO**, one of the prominent oxysterols found in the cells and tissues reported here, suggest that it has important roles in different signaling pathways (27). Our previous studies indicate that **DHCEO** downregulates *Ki67*, a marker of cell proliferation, and *Egr1* (27). **DHCEO** also regulates genes involved in lipid biosynthesis such as *Hmgcr*, *Dhcr7*, and *SQS*, as well as other genes, including *Prr13*, *Adam19*, and *Snag1*. In an earlier publication by Gaoua et al. (70), it was reported that a UV-photooxidation product mixture of 7-DHC induced growth retardation in cultured rat embryos and the antioxidant α-tocopherol reduced the toxicity of this product mixture. Notably, we also found that purified 7-DHC photooxidation products are toxic to a control Neuro2a cell line at μM concentration range (27).

The observation that a known antioxidant can suppress the formation of **DHCEO** in the SLOS HF cell line not only further validates the notion that **DHCEO** is a good biomarker for 7-DHC oxidation, but may also open the possibility of a new therapeutic approach to SLOS. Inhibition of the formation of 7-DHC-derived oxysterols may alleviate some of the deleterious effects exerted by these oxysterols, which could eventually lead to improved outcomes for SLOS patients. The precise mechanism by which antioxidants attenuate the formation of 7-DHC oxysterols has not been established. Indeed, they could inhibit both the free radical chain mechanism as well as oxygenase enzymes that operate via higher valence metals (65, 71, 72). But regardless of the mechanism by which the pyrimidinol antioxidant studied here exerts its effect, the net result is a reduction of formation of toxic oxysterol products. A previous study by Tint et al. (39) suggested that there is no correlation between the level of 7-DHC and the severity of the SLOS phenotype. Thus, it would be interesting to examine the correlation between the level of 7-DHC-derived oxysterol and the SLOS phenotypes as different individuals may have different antioxidant capability.

TABLE 3. Normalized levels of **DHCEO** (ng/mg protein) formed from 5 μM **1** (epoxide) or **2** (triol) in the presence of different cell lines over 24 h

	HF-control		HF-SLOS		Neuro2a-control	
Substrate compound	1	2	1	2	1	2
DHCEO in Cells (ng/mg)	238 ± 19	717 ± 31	204 ± 26	808 ± 25	2630 ± 184	2242 ± 164
DHCEO in medium (ng/mg)	414 ± 47	1911 ± 291	324 ± 42	1058 ± 46	1240 ± 56	1470 ± 36
Total **DHCEO** (ng/mg)	653 ± 33	2629 ± 316	527 ± 68[a]	1865 ± 69[a]	3870 ± 190[b]	3712 ± 157[a]
Ratio of **DHCEO**[c]	4		3.5		1	

Regular FBS was used here; no **DHCEO** detected in any system in the absence of compound **1** or **2**; statistical analyses were performed against corresponding HF-control.
[a] $p < 0.05$.
[b] $p < 0.0005$.
[c] Ratio of total **DHCEO** formed from triol **2** to that formed from epoxide **1**.

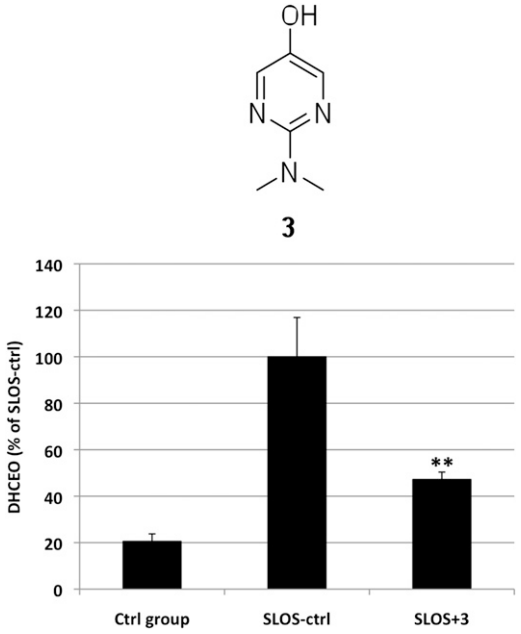

Fig. 8. Effect of 10 μM antioxidant **3** on the level of **DHCEO** in SLOS HFs. **, $p < 0.005$ relative to SLOS-ctrl.

In conclusion, multiple new oxysterols were found in SLOS cell models and in tissues from a mouse model for SLOS. A novel oxysterol, **DHCEO**, was identified in these cells and tissues. Levels of **DHCEO**, 7-DHC, and Chol were quantified by isotope dilution MS using synthetic deuterated (d_7) standards. *Dhcr7*-deficient Neuro2a cells, SLOS HFs, and brain tissues from *Dhcr7*-KO mice all show elevated levels of this oxysterol. Incubation experiments suggest that 5α,6α-epoxycholest-7-en-3β-ol (**1**), a primary free radical oxidation product, and 7-cholesten-3β,5α,6β-triol (**2**) are possible precursors to **DHCEO** in cells and tissues. A pyrimidinol antioxidant was found to effectively suppress the formation of **DHCEO** in the SLOS HF cell lines, which opens the possibility of a new therapeutic approach to SLOS. The good correlation between levels of **DHCEO** and 7-DHC, combined with the suppression of the formation of **DHCEO** by antioxidants, suggest that **DHCEO** is a good biomarker for 7-DHC oxidation.

REFERENCES

1. Irons, M., E. R. Elias, G. Salen, G. S. Tint, and A. K. Batta. 1993. Defective cholesterol biosynthesis in Smith-Lemli-Opitz syndrome. *Lancet.* **341:** 1414.
2. Tint, G. S., M. Irons, E. R. Elias, A. K. Batta, R. Frieden, T. S. Chen, and G. Salen. 1994. Defective cholesterol biosynthesis associated with the Smith-Lemli-Opitz syndrome. *N. Engl. J. Med.* **330:** 107–113.
3. Fitzky, B. U., F. F. Moebius, H. Asaoka, H. Waage-Baudet, L. Xu, G. Xu, N. Maeda, K. Kluckman, S. Hiller, H. Yu, et al. 2001. 7-Dehydrocholesterol-dependent proteolysis of HMG-CoA reductase suppresses sterol biosynthesis in a mouse model of Smith-Lemli-Opitz/RSH syndrome. *J. Clin. Invest.* **108:** 905–915.
4. Krakowiak, P. A., N. A. Nwokoro, C. A. Wassif, K. P. Battaile, M. J. Nowaczyk, W. E. Connor, C. Maslen, R. D. Steiner, and F. D. Porter. 2000. Mutation analysis and description of sixteen RSH/Smith-Lemli-Opitz syndrome patients: polymerase chain reaction-based assays to simplify genotyping. *Am. J. Med. Genet.* **94:** 214–227.
5. Waterham, H. R. 2002. Inherited disorders of cholesterol biosynthesis. *Clin. Genet.* **61:** 393–403.
6. Sikora, D., K. Pettit-Kekel, J. Penfield, L. Merkens, and R. Steiner. 2006. The near universal presence of autism spectrum disorders in children with Smith–Lemli–Opitz syndrome. *Am. J. Med. Genet.* **140:** 1511–1518.
7. Porter, F. D., and G. E. Herman. 2010. Malformation syndromes caused by disorders of cholesterol synthesis. *J. Lipid Res.* **52:** 6–34.
8. Kelley, R. I., and R. C. Hennekam. 2000. The Smith-Lemli-Opitz syndrome. *J. Med. Genet.* **37:** 321–335.
9. Porter, F. D. 2003. Human malformation syndromes due to inborn errors of cholesterol synthesis. *Curr. Opin. Pediatr.* **15:** 607–613.
10. Bukelis, I., F. D. Porter, A. W. Zimmerman, and E. Tierney. 2007. Smith-Lemli-Opitz syndrome and autism spectrum disorder. *Am. J. Psychiatry.* **164:** 1655–1661.
11. Xu, L., T. A. Davis, and N. A. Porter. 2009. Rate constants for peroxidation of polyunsaturated fatty acids and sterols in solution and in liposomes. *J. Am. Chem. Soc.* **131:** 13037–13044.
12. Xu, L., Z. Korade, and N. A. Porter. 2010. Oxysterols from free radical chain oxidation of 7-dehydrocholesterol: product and mechanistic studies. *J. Am. Chem. Soc.* **132:** 2222–2232.
13. Vejux, A., and G. Lizard. 2009. Cytotoxic effects of oxysterols associated with human diseases: induction of cell death (apoptosis and/or oncosis), oxidative and inflammatory activities, and phospholipidosis. *Mol. Aspects Med.* **30:** 153–170.
14. Schroepfer, G. J., Jr. 2000. Oxysterols: modulators of cholesterol metabolism and other processes. *Physiol. Rev.* **80:** 361–554.
15. Janowski, B. A., P. J. Willy, T. R. Devi, J. R. Falck, and D. J. Mangelsdorf. 1996. An oxysterol signalling pathway mediated by the nuclear receptor LXR alpha. *Nature.* **383:** 728–731.
16. Repa, J. J., G. Liang, J. Ou, Y. Bashmakov, J. M. Lobaccaro, I. Shimomura, B. Shan, M. S. Brown, J. L. Goldstein, and D. J. Mangelsdorf. 2000. Regulation of mouse sterol regulatory element-binding protein-1c gene (SREBP-1c) by oxysterol receptors, LXRalpha and LXRbeta. *Genes Dev.* **14:** 2819–2830.
17. Venkateswaran, A., B. A. Laffitte, S. B. Joseph, P. A. Mak, D. C. Wilpitz, P. A. Edwards, and P. Tontonoz. 2000. Control of cellular cholesterol efflux by the nuclear oxysterol receptor LXR alpha. *Proc. Natl. Acad. Sci. USA.* **97:** 12097–12102.
18. Javitt, N. B. 2004. Oxysteroids: a new class of steroids with autocrine and paracrine functions. *Trends Endocrinol. Metab.* **15:** 393–397.
19. Brown, A. J., and W. Jessup. 2009. Oxysterols: sources, cellular storage and metabolism, and new insights into their roles in cholesterol homeostasis. *Mol. Aspects Med.* **30:** 111–122.
20. Yachnin, S., and R. Hsu. 1980. Inhibition of human lymphocyte transformation by oxygenated sterol compounds. *Cell. Immunol.* **51:** 42–54.
21. Moog, C., B. Luu, J. P. Beck, L. Italiano, and P. Bischoff. 1988. Studies on the immunosuppressive properties of 7,25-dihydroxycholesterol–I. Reduction of interleukin production by treated lymphocytes. *Int. J. Immunopharmacol.* **10:** 511–518.
22. Moog, C., B. Luu, A. Altmeyer, and P. Bischoff. 1989. Studies on the immunosuppressive properties of 7,25 dihydroxycholesterol–II. Effects on early steps of T-cell activation. *Int. J. Immunopharmacol.* **11:** 559–565.
23. Moog, C., Y. H. Ji, C. Waltzinger, B. Luu, and P. Bischoff. 1990. Studies on the immunological properties of oxysterols: in vivo actions of 7,25-dihydroxycholesterol upon murine peritoneal cells. *Immunology.* **70:** 344–350.
24. Kha, H. T., B. Basseri, D. Shouhed, J. Richardson, S. Tetradis, T. J. Hahn, and F. Parhami. 2004. Oxysterols regulate differentiation of mesenchymal stem cells: pro-bone and anti-fat. *J. Bone Miner. Res.* **19:** 830–840.
25. Dwyer, J. R., N. Sever, M. Carlson, S. F. Nelson, P. A. Beachy, and F. Parhami. 2007. Oxysterols are novel activators of the hedgehog signaling pathway in pluripotent mesenchymal cells. *J. Biol. Chem.* **282:** 8959–8968.
26. Javitt, N. B. 2008. Oxysterols: novel biologic roles for the 21st century. *Steroids.* **73:** 149–157.
27. Korade, Z., L. Xu, R. Shelton, and N. A. Porter. 2010. Biological activities of 7-dehydrocholesterol-derived oxysterols: implications for Smith-Lemli-Opitz syndrome. *J. Lipid Res.* **51:** 3259–3269.
28. Akin, D., D. H. Manier, E. Sanders-Bush, and R. C. Shelton. 2005. Signal transduction abnormalities in melancholic depression. *Int. J. Neuropsychopharmacol.* **8:** 5–16.
29. Sassone, J., C. Colciago, G. Cislaghi, V. Silani, and A. Ciammola. 2009. Huntington's disease: the current state of research with peripheral tissues. *Exp. Neurol.* **219:** 385–397.
30. del Hoyo, P. M., A. M. P. Garcia-Redondo, F. B. de Bustos, J. A. M. P. Molina, Y. M. Sayed, H. M. P. Alonso-Navarro, L. M. P. Caballero,

J. M. P. Arenas, J. A. M. P. Agundez, and F. J. M. P. Jimenez-Jimenez. 2010. Oxidative stress in skin fibroblasts cultures from patients with Parkinson's disease. *BMC Neurol.* **10:** 95.
31. Squitieri, F., A. Falleni, M. Cannella, S. Orobello, F. Fulceri, P. Lenzi, and F. Fornai. 2010. Abnormal morphology of peripheral cell tissues from patients with Huntington disease. *J. Neural Transm.* **117:** 77–83.
32. Honda, A., G. S. Tint, G. Salen, A. K. Batta, T. S. Chen, and S. Shefer. 1995. Defective conversion of 7-dehydrocholesterol to cholesterol in cultured skin fibroblasts from Smith-Lemli-Opitz Syndrome homozygotes. *J. Lipid Res.* **36:** 1595–1601.
33. Honda, A., G. S. Tint, G. Salen, R. I. Kelley, M. Honda, A. K. Batta, T. S. Chen, and S. Shefer. 1997. Sterol concentrations in cultured Smith-Lemli-Opitz syndrome skin fibroblasts: diagnosis of a biochemically atypical case of the syndrome. *Am. J. Med. Genet.* **68:** 282–287.
34. Fu, R., N. M. Yanjanin, S. Bianconi, W. J. Pavan, and F. D. Porter. 2010. Oxidative stress in Niemann-Pick disease, type C. *Mol. Genet. Metab.* **101:** 214–218.
35. De Fabiani, E., D. Caruso, M. Cavaleri, M. Galli Kienle, and G. Galli. 1996. Cholesta-5,7,9(11)-trien-3 beta-ol found in plasma of patients with Smith-Lemli-Opitz syndrome indicates formation of sterol hydroperoxide. *J. Lipid Res.* **37:** 2280–2287.
36. Fliesler, S. J., N. S. Peachey, M. J. Richards, B. A. Nagel, and D. K. Vaughan. 2004. Retinal degeneration in a rodent model of Smith-Lemli-Opitz syndrome: electrophysiologic, biochemical, and morphologic features. *Arch. Ophthalmol.* **122:** 1190–1200.
37. Richards, M. J., B. A. Nagel, and S. J. Fliesler. 2006. Lipid hydroperoxide formation in the retina: correlation with retinal degeneration and light damage in a rat model of Smith-Lemli-Opitz syndrome. *Exp. Eye Res.* **82:** 538–541.
38. Wassif, C. A., P. Zhu, L. Kratz, P. A. Krakowiak, K. P. Battaile, F. F. Weight, A. Grinberg, R. D. Steiner, N. A. Nwokoro, R. I. Kelley, et al. 2001. Biochemical, phenotypic and neurophysiological characterization of a genetic mouse model of RSH/Smith-Lemli-Opitz syndrome. *Hum. Mol. Genet.* **10:** 555–564.
39. Tint, G. S., G. Salen, A. K. Batta, S. Shefer, M. Irons, E. R. Elias, D. N. Abuelo, V. P. Johnson, M. Lambert, R. Lutz, et al. 1995. Correlation of severity and outcome with plasma sterol levels in variants of the Smith-Lemli-Opitz syndrome. *J. Pediatr.* **127:** 82–87.
40. Tint, G. S., H. Yu, Q. Shang, G. Xu, and S. B. Patel. 2006. The use of the *Dhcr7* knockout mouse to accurately determine the origin of fetal sterols. *J. Lipid Res.* **47:** 1535–1541.
41. Waage-Baudet, H., J. M. Lauder, D. B. Dehart, K. Kluckman, S. Hiller, G. S. Tint, and K. K. Sulik. 2003. Abnormal serotonergic development in a mouse model for the Smith-Lemli-Opitz syndrome: implications for autism. *Int. J. Dev. Neurosci.* **21:** 451–459.
42. Jiang, X. S., C. A. Wassif, P. S. Backlund, L. Song, L. A. Holtzclaw, Z. Li, A. L. Yergey, and F. D. Porter. 2010. Activation of Rho GTPases in Smith-Lemli-Opitz syndrome: pathophysiological and clinical implications. *Hum. Mol. Genet.* **19:** 1347–1357.
43. Dietschy, J. M., and S. D. Turley. 2001. Cholesterol metabolism in the brain. *Curr. Opin. Lipidol.* **12:** 105–112.
44. Dietschy, J. M., and S. D. Turley. 2004. Thematic review series: brain lipids. Cholesterol metabolism in the central nervous system during early development and in the mature animal. *J. Lipid Res.* **45:** 1375–1397.
45. Yablonskaya, E., and M. Segal. 1973. Synthesis of 7-dehydrocholesterol acetate. *Chem. Nat. Compd.* **9:** 708–709.
46. Pearson, A., Y. Chen, G. Han, S. Hsu, and T. Ray. 1985. A new method for the oxidation of alkenes to enones: an efficient synthesis of △ 5–7-oxo steroids. *J. Chem. Soc. Perkins Trans.* **I:** 267–273.
47. Piccialli, V., D. Sica, and D. Smaldone. 1994. Reaction of 7-dehydrocholesteryl acetate with Ru04. First isolation of a cyclic ruthenium (VI) diester. *Tetrahedron Lett.* **35:** 7093–7096.
48. van Leeuwen, S. M., L. Hendriksen, and U. Karst. 2004. Determination of aldehydes and ketones using derivatization with 2,4-dinitrophenylhydrazine and liquid chromatography-atmospheric pressure photoionization-mass spectrometry. *J. Chromatogr. A.* **1058:** 107–112.
49. Andreoli, R., P. Manini, M. Corradi, A. Mutti, and W. M. Niessen. 2003. Determination of patterns of biologically relevant aldehydes in exhaled breath condensate of healthy subjects by liquid chromatography/atmospheric chemical ionization tandem mass spectrometry. *Rapid Commun. Mass Spectrom.* **17:** 637–645.
50. Yamashita, K., M. Okuyama, Y. Watanabe, S. Honma, S. Kobayashi, and M. Numazawa. 2007. Highly sensitive determination of estrone and estradiol in human serum by liquid chromatography-electrospray ionization tandem mass spectrometry. *Steroids.* **72:** 819–827.
51. Yen, T. Y., B. S. Inbaraj, J. T. Chien, and B. H. Chen. 2010. Gas chromatography-mass spectrometry determination of conjugated linoleic acids and cholesterol oxides and their stability in a model system. *Anal. Biochem.* **400:** 130–138.
52. Aringer, L., and P. Eneroth. 1974. Formation and metabolism in vitro of 5,6-epoxides of cholesterol and beta-sitosterol. *J. Lipid Res.* **15:** 389–398.
53. Pulfer, M. K., and R. C. Murphy. 2004. Formation of biologically active oxysterols during ozonolysis of cholesterol present in lung surfactant. *J. Biol. Chem.* **279:** 26331–26338.
54. Murphy, R. C., and K. M. Johnson. 2008. Cholesterol, reactive oxygen species, and the formation of biologically active mediators. *J. Biol. Chem.* **283:** 15521–15525.
55. Watabe, T., and T. Sawahata. 1979. Biotransformation of cholesterol to cholestane-3beta,5alpha,6beta-triol via cholesterol alpha-epoxide (5alpha,6alpha-epoxycholestan-3beta-ol) in bovine adrenal cortex. *J. Biol. Chem.* **254:** 3854–3860.
56. Watabe, T., M. Kanai, M. Isobe, and N. Ozawa. 1981. The hepatic microsomal biotransformation of delta 5-steroids to 5 alpha, 6 beta-glycols via alpha- and beta-epoxides. *J. Biol. Chem.* **256:** 2900–2907.
57. Gumulka, J., J. Pyrek, and L. Smith. 1982. Interception of discrete oxygen species in aqueous media by cholesterol: formation of cholesterol epoxides and secosterols. *Lipids.* **17:** 197–203.
58. Smith, L. L. 1987. Cholesterol autoxidation 1981–1986. *Chem. Phys. Lipids.* **44:** 87–125.
59. Bach, R. D., and J. W. Knight. 1981. Epoxidation of olefins by hydrogen peroxide-acetonitrile: cis-cyclooctene oxide. *Org. Synth.* **60:** 63–66.
60. Michaud, D. P., N. T. Nashed, and D. M. Jerina. 1985. Stereoselective synthesis and solvolytic behavior of the isomeric 7-dehydrocholesterol 5,6-oxides. *J. Org. Chem.* **50:** 1835–1840.
61. Matsumoto, A., and H. Higashi. 2000. Convenient synthesis of polymers containing labile bonds in the main chain by radical alternating copolymerization of alkyl sorbates with oxygen. *Macromolecules.* **33:** 1651–1655.
62. Schneider, C., W. E. Boeglin, H. Yin, N. A. Porter, and A. R. Brash. 2008. Intermolecular peroxyl radical reactions during autoxidation of hydroxy and hydroperoxy arachidonic acids generate a novel series of epoxidized products. *Chem. Res. Toxicol.* **21:** 895–903.
63. Wijtmans, M., D. A. Pratt, L. Valgimigli, G. A. DiLabio, G. F. Pedulli, and N. A. Porter. 2003. 6-Amino-3-pyridinols: towards diffusion-controlled chain-breaking antioxidants. *Angew. Chem. Int. Ed.* **42:** 4370–4373.
64. Wijtmans, M., D. A. Pratt, J. Brinkhorst, R. Serwa, L. Valgimigli, G. F. Pedulli, and N. A. Porter. 2004. Synthesis and reactivity of some 6-substituted-2,4-dimethyl-3-pyridinols, a novel class of chain-breaking antioxidants. *J. Org. Chem.* **69:** 9215–9223.
65. Nam, T. G., S. J. Nara, I. Zagol-Ikapitte, T. Cooper, L. Valgimigli, J. A. Oates, N. A. Porter, O. Boutaud, and D. A. Pratt. 2009. Pyridine and pyrimidine analogs of acetaminophen as inhibitors of lipid peroxidation and cyclooxygenase and lipoxygenase catalysis. *Org. Biomol. Chem.* **7:** 5103–5112.
66. Omata, Y., Y. Saito, Y. Yoshida, B. S. Jeong, R. Serwa, T. G. Nam, N. A. Porter, and E. Niki. 2010. Action of 6-amino-3-pyridinols as novel antioxidants against free radicals and oxidative stress in solution, plasma, and cultured cells. *Free Radic. Biol. Med.* **48:** 1358–1365.
67. Wassif, C. A., J. Yu, J. Cui, F. D. Porter, and N. B. Javitt. 2003. 27-Hydroxylation of 7- and 8-dehydrocholesterol in Smith-Lemli-Opitz syndrome: a novel metabolic pathway. *Steroids.* **68:** 497–502.
68. Holick, M. F., J. E. Frommer, S. C. McNeill, N. M. Richtand, J. W. Henley, and J. T. Potts, Jr. 1977. Photometabolism of 7-dehydrocholesterol to previtamin D3 in skin. *Biochem. Biophys. Res. Commun.* **76:** 107–114.
69. Song, B. L., N. B. Javitt, and R. A. DeBose-Boyd. 2005. Insig-mediated degradation of HMG CoA reductase stimulated by lanosterol, an intermediate in the synthesis of cholesterol. *Cell Metab.* **1:** 179–189.
70. Gaoua, W., F. Chevy, C. Roux, and C. Wolf. 1999. Oxidized derivatives of 7-dehydrocholesterol induce growth retardation in cultured rat embryos: a model for antenatal growth retardation in the Smith-Lemli-Opitz syndrome. *J. Lipid Res.* **40:** 456–463.
71. Chun, Y. J., S. Y. Ryu, T. C. Jeong, and M. Y. Kim. 2001. Mechanism-based inhibition of human cytochrome P450 1A1 by rhapontigenin. *Drug Metab. Dispos.* **29:** 389–393.
72. Chang, T. K., J. Chen, and W. B. Lee. 2001. Differential inhibition and inactivation of human CYP1 enzymes by trans-resveratrol: evidence for mechanism-based inactivation of CYP1A2. *J. Pharmacol. Exp. Ther.* **299:** 874–882.